Isotope identity experiments in JET-ILW with H and D L-mode plasmas

Isotope identity experiments in JET-ILW with H and D L-mode plasmas

CF Maggi[1], H Weisen[2], FJ Casson[1], F Auriemma[3], R Lorenzini[3], H Nordman[4], E Delabie[5], F Eriksson[4], J Flanagan[1], D Keeling[1], D King[1], L Horvath[6], S Menmuir[1], A Salmi[7], G Sips[8], T Tala[7], I Voitsekhovich[1] and JET Contributors*

EUROfusion Consortium, JET, Culham Science Centre, Abingdon, OX14 3DB, UK
[1]CCFE, Culham Science Centre, Abingdon OX14 3DB, UK
[2]SPC, Ecole Polytechnique Federale de Lausanne, Switzerland
[3]Consorzio RFX, Corso Stati Uniti 4, I-35127 Padova, Italy
[4]Chalmers University of Technology, Göteborg, Sweden
[5]Oak Ridge National Laboratory, Oak Ridge, Tennessee, United States of America
[6]York Plasma Institute, Department of Physics, University of York, York YO10 5DD, UK
[7] VTT, FI-02044 VTT, Espoo, Finland
[8]European Commission, Brussels, Belgium
*(*) See the author list of X Litaudon et al. 2017 Nucl. Fusion **57** 102001*

Abstract. NBI-heated L-mode plasmas have been obtained in JET with the Be/W ITER-like wall (JET-ILW) in H and D, with matched profiles of the dimensionless plasma parameters, ρ*, ν*, β and q in the plasma core confinement region and same T_i/T_e and Z_{eff}. The achieved isotope identity indicates that the confinement scale invariance principle is satisfied in the core confinement region of these plasmas, where the dominant instabilities are Ion Temperature Gradient (ITG) modes. The dimensionless thermal energy confinement time, $\Omega_i\ \tau_{E,th}$, and the scaled core plasma heat diffusivity, $A\chi_{eff}/B_{T,}$ are identical in H and D within error bars, indicating lack of isotope mass dependence of the dimensionless L-mode thermal energy confinement time in JET-ILW. Predictive flux driven simulations with JETTO-TGLF of the H and D identity pair is in very good agreement with experiment for both isotopes: the stiff core heat transport, typical of JET-ILW NBI heated L-modes, overcomes the local gyro-Bohm scaling of gradient-driven TGLF, explaining the lack of isotope mass dependence in the confinement region of these plasmas. The effect of *ExB* shearing on the predicted heat and particle transport channels is found to be negligible for these low beta and low momentum input plasmas.

1. Introduction

Dimensionless identity experiments test the invariance of plasma physics to changes in the dimensional plasma parameters, e.g. density and temperature, when the canonical dimensionless plasma physics parameters ρ*, ν*, β, *q*, ... are conserved [1] [2]. Plasmas with dissimilar dimensional parameters but identical dimensionless parameters should have identical transport, with the appropriate normalization to make it dimensionless [2]. However, conditions at the plasma boundary, such as influx of neutral particles, may introduce additional physics, potentially invalidating this approach. It is therefore important to test experimentally the validity of this principle, which is at the heart of extrapolations of plasma transport properties to future devices. $\rho^* \sim \sqrt{(A\ T_i)} / (a\ B_T)$ is the Larmor radius of thermal ions normalized to the plasma minor radius (with $A = m_i/m_p$ the isotope ion mass

normalized to the proton mass, T_i the ion temperature, a the plasma minor radius and B_T the toroidal magnetic field on axis); $\beta \sim n\ T\ /\ B^2$ is the plasma pressure normalized to the magnetic pressure (with n the plasma density); $\nu^* \sim n_e\ R\ Z_{eff}\ /\ T_e^2$ is the electron-ion collision frequency normalized to the thermal ion bounce frequency (with Z_{eff} the plasma effective charge, R the major radius); $q \sim B\ /\ (I\ R)$ is the safety factor (with I the plasma current). The inverse aspect ratio $\varepsilon = a/R$ and κ, the ratio of plasma height and width, also need to be constant. Following the literature, e.g. [2], the dimensionless thermal energy confinement time has the general form:

$$\Omega_i\ \tau_{E,th} = F\ (\rho^*,\ \nu^*,\ \beta,\ \ldots) \qquad (1)$$

with $\Omega_i \sim eB/A$ the ion cyclotron frequency (e is the particle charge). Typically, the function F is expressed in terms of the product of power laws of the plasma dimensionless parameters [2]:

$$\Omega_i\ \tau_{E,th} \sim (\rho^{*-\alpha_\rho}\ \beta^{-\alpha_\beta}\ \nu^{*-\alpha_\nu}\ q^{-\alpha q}\ A^{-\alpha A}\ \ldots) \qquad (2)$$

The favourable dependence of energy and particle transport on the main ion isotope mass is of fundamental interest for the understanding of turbulent transport and, therefore, for accurate predictions of confinement from present day tokamak experiments to future burning devices. While future experiments, such as ITER, will operate in Deuterium-Tritium mixtures, today's tokamak experiments typically use a single hydrogen isotope (predominantly deuterium). Complete theoretical understanding of the favourable isotopic dependence of transport and confinement still remains elusive, but recently new impetus was injected in this field of research by a series of isotope experiments in JET with the ITER-like Be/W wall (JET-ILW) in preparation for a second D-T experiment. While most studies investigate the isotope scaling of confinement in dimensional experiments, we follow here the Connor-Taylor scale invariance approach [1]. Isotope identity experiments exploit the change in isotope ion mass to obtain plasmas with identical dimensionless profiles in the same tokamak. In order to keep ρ^*, β, ν^* and q profiles fixed when also varying the isotope mass, the plasma current, toroidal magnetic field and the density and temperature must scale, respectively, as: I_P, $B_T \sim A^{3/4}$; $n \sim A$ and $T \sim \sqrt{A}$ [3], [4]. Accordingly, for equal scaled energy confinement times $B\ \tau_{E,th}/A$, the absorbed input power must scale as $P_{abs} = W_{th}\ /\ \tau_{E,th} \sim B_T^{5/3}$ (or $\sim A^{5/4}$), where W_{th} is the thermal stored energy, and the heat diffusivity must scale as $\chi \sim B/A$, with χ defined in terms of the temperature gradient and the heat flux $q = -\ n\ \chi\ \nabla T$.

An isotope identity experiment was first carried out in the JET tokamak, with C wall (JET-C). Type I ELMy H-modes were obtained in H (1MA/1T, H-NBI) and D (1.7MA/1.7T, D-NBI), with average plasma triangularity $\delta = 0.3$, with matching ρ^*, ν^*, β and q profiles [3]. Remarkably, it was found that the scaled thermal energy confinement time, $B\ \tau_{E,th}/A$, the scaled ELM frequency, $A\ f_{ELM}/B$ and the scaled sawtooth frequency, $A\ f_{saw}/B$, were all matched within error bars in the H and D plasmas, indicating that the invariance principle was satisfied throughout the entire plasma radius, despite the different physical processes in the plasma centre, core confinement and edge regions [3]. We note that the match in scaled ELM frequency and scaled sawtooth frequency in H and D is not in the original theory of [1] and could have been fortuitous in the experiments reported in [3]. We also note that in the JET-C experiments the plasma isotope purity in H, $n_H / (n_H + n_D) = 0.89$, was not as good as can be obtained in JET-ILW (see section 3), the Be/W metallic wall having demonstrated significant reduction in main fuel retention [4] and faster isotope wall change-over.

When the isotope identity has been achieved, e.g. in the H and D discharge pair of [3], one can extract the value of the exponent α_A yielding the isotope mass scaling of the dimensionless thermal energy confinement time $\Omega_i\, \tau_{E,th} \sim A^{-\alpha A}$, since the quantity $(\rho^{*-\alpha\rho}\ \beta^{-\alpha\beta}\ \nu^{*-\alpha\nu}\ q^{-\alpha q}\ \ldots)$ in equation (2) is a constant. The JET-C isotope identity experiment in H and D in type I ELMy H-mode yielded a weak, positive isotope mass scaling $\Omega_i\, \tau_{E,th} \sim A^{0.14}$ [2]. This was found to be largely consistent with the lack of mass dependence of (dimensional) global energy confinement time, $\tau_{E,th} \sim A^{0.03\pm0.10}$, obtained in JET-C type I ELMy H-modes in H, D, T and D-T at similar density and input power. The latter resulted from the combination of strong, positive mass dependence for W_{PED} (pedestal stored energy) and weak, negative mass dependence in the plasma core, $\tau_{th,core} \sim A^{-0.16}$ [5]. The scaled local heat diffusivities from power balance, $A\ \chi_{eff}/B$, were also found to be similar in H and D, within experimental uncertainties in the TRANSP power balance, with χ_{eff} the one-fluid thermal diffusivity, since a species resolved power balance analysis was not possible in [3].

The isotope identity technique was revisited in recent experiments with H and D plasmas in JET-ILW. Additionally, compared to the earlier JET-C experiments, improved core and edge electron profile diagnosis with HRTS is available [6]. This paper reports on the experiments in the L-mode regime: the experimental results and interpretative TRANSP analysis are described in Section 2, predictive core plasma transport modelling is presented in Section 3, followed by conclusions and outlook in Section 4. Isotope identity experiments in H and D type I ELMy H-modes were also performed but will be reported separately,

pending further experiments, planned for the upcoming JET-ILW campaign, aimed at optimizing the required profile matches in H-mode.

2. JET-ILW L-mode isotope identity experiment and interpretative analysis

An L-mode isotope identity pair was achieved in JET-ILW at I_P/B_T = 2.46MA/2.95T in D and 1.44MA/1.74T in H, q_{95} = 3.4, low plasma triangularity δ = 0.2. The chosen divertor configuration was with both strike points on the divertor vertical targets, as shown in Figure 1, in order to maximize the L-H power threshold at a given plasma density and toroidal magnetic field [7] and thus maximize the L-mode domain, in particular in view of comparison with Tritium discharges, which are foreseen in future JET-ILW experiments. The auxiliary heating was provided by neutral beam injection (NBI), with D-NBI (beam energy: 82-91 keV) and H-NBI (beam energy: 64-71 keV), respectively. The excellent isotope purity in these plasmas, $n_H/(n_H + n_D) > 98$ %, is a feature of the ITER-like Be/W wall and a result of the long (6-week) H experimental campaign. The $n_H/(n_H + n_D)$ ratio was continuously monitored by edge (divertor and midplane) Balmer-α spectroscopy, sub-divertor neutral gas analysis, a core neutral particle analyser and total neutron rate (the latter was particularly useful as a measure of plasma core $n_H/(n_H + n_D)$ fractions during mixed H/D plasma experiments). After the last introduction of D (by pellets) into plasma discharges, the D concentration dropped to 1% within three H plasma discharges and remained constant at this level for the full H campaign [8].

Figures 1 a, b show the good match in the scaled kinetic profiles n_e/A and $T_e/\sqrt{A}$, measured by HRTS, for the H and D discharge pair. The data are composite profiles in the steady time intervals chosen for the analysis, which correspond to 10 x $\tau_{E,th}$. For both H and D plasmas, $T_i = T_e$ within uncertainties of the T_i measurements (±10%) from CXRS [9] (obtained from C VI, n = 8-7 transition for the D pulse and from Ne X, n = 11-10 transition for the H pulse, which used trace Ne puffs to enable core CXRS measurements). The normalized density and temperature gradient lengths, $R/L_{ne} = - R (dn_e/dr)/n_e$ and $R/L_{Te} = - R (dT_e/dr)/T_e$, corresponding to the profiles of Figure 1 are derived from the fits to the composite profile data and are compared in Figure 2 a, b, showing good agreement in H and D, especially for R/L_{Te}.

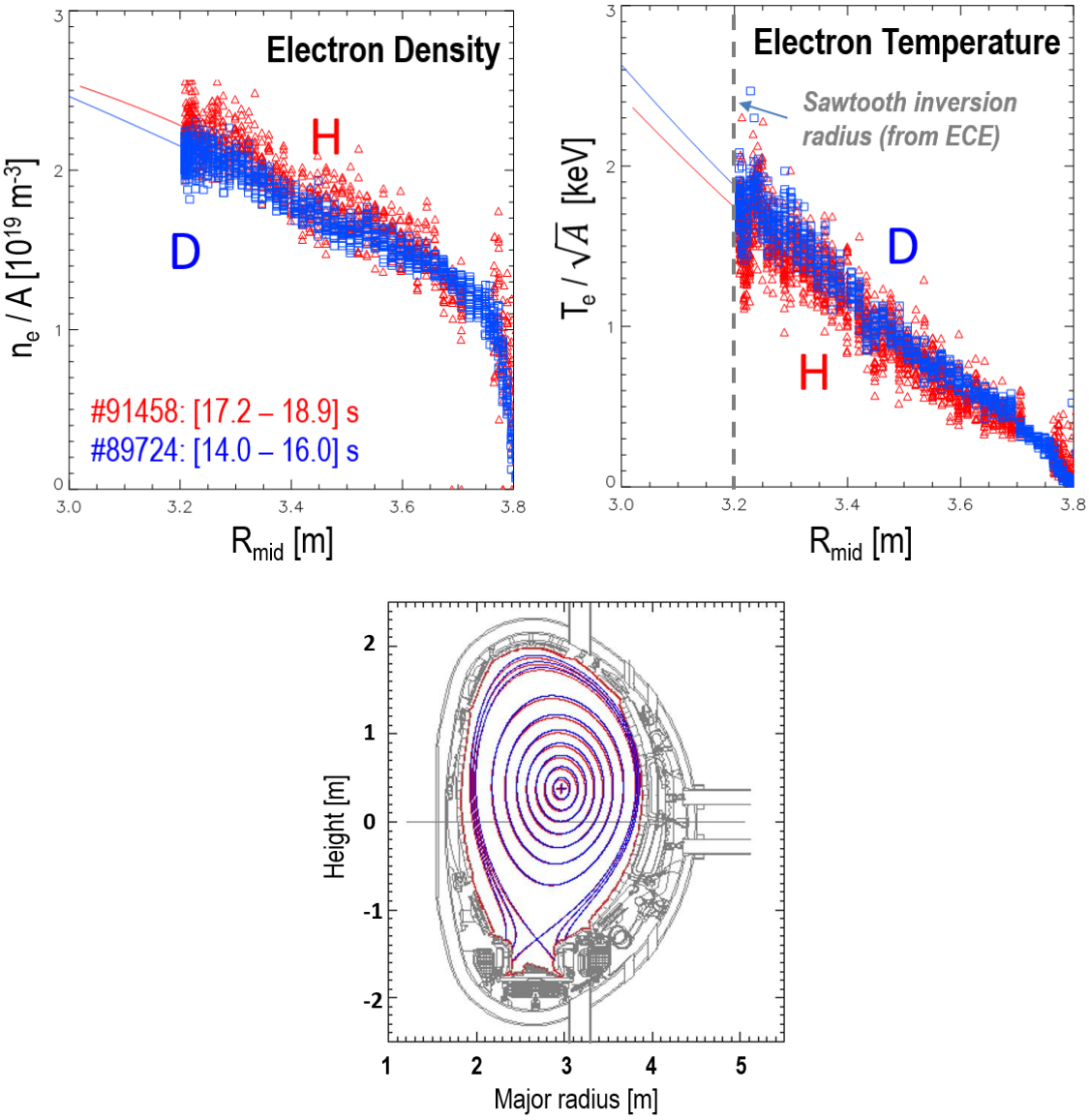

Figure 1. *Scaled n_e (a) and T_e (b) profiles from HRTS for the JET-ILW L-mode isotope identity pair in H (#91458, red) and D (#89724, blue) versus R_{mid}, the major radius at z of magnetic axis. The data are composite profiles in the steady time interval analysed (noted in Figure 1a) and the solid lines correspond to the fits to the data. T_i = T_e within experimental uncertainties of the T_i measurements from CXRS (±10%). (c): Matched plasma equilibria in H and D, showing the divertor configuration with both strike points on the vertical targets.*

The profiles of the matched dimensionless plasma parameters of the H and D L-mode pair are shown in Figure 3. The normalized ion Larmor radius ρ*, the normalized collisionality ν* and the normalized thermal pressure β profiles have been calculated using the following definitions:

$$\rho^* = 4.57 \times 10^{-3} (A\, T_i)^{1/2} / (a\, B_T), \quad (3)$$

$$\nu^* = 0.0011\, n_e\, R\, q_{95}\, Z_{eff} / (\varepsilon^{3/2}\, T_e^2) \quad (4)$$

$$\beta = (p_e + p_i)/(B_T^2/2\mu_0) \quad (5)$$

where B_T [T] is the toroidal magnetic field on axis, T_i and T_e are in keV, n_e is in 10^{19} m^{-3} and p_e and p_i are the electron and ion thermal pressure profiles, respectively. The ion thermal pressure is calculated from $T_i = T_e$ and $n_i = n_e\,(5 - Z_{eff})/4$, assuming Beryllium as the main impurity. The q-profile is matched by keeping constant plasma shape and scaling I_P and B_T proportionally to $A^{3/4}$, as introduced in Section 1.

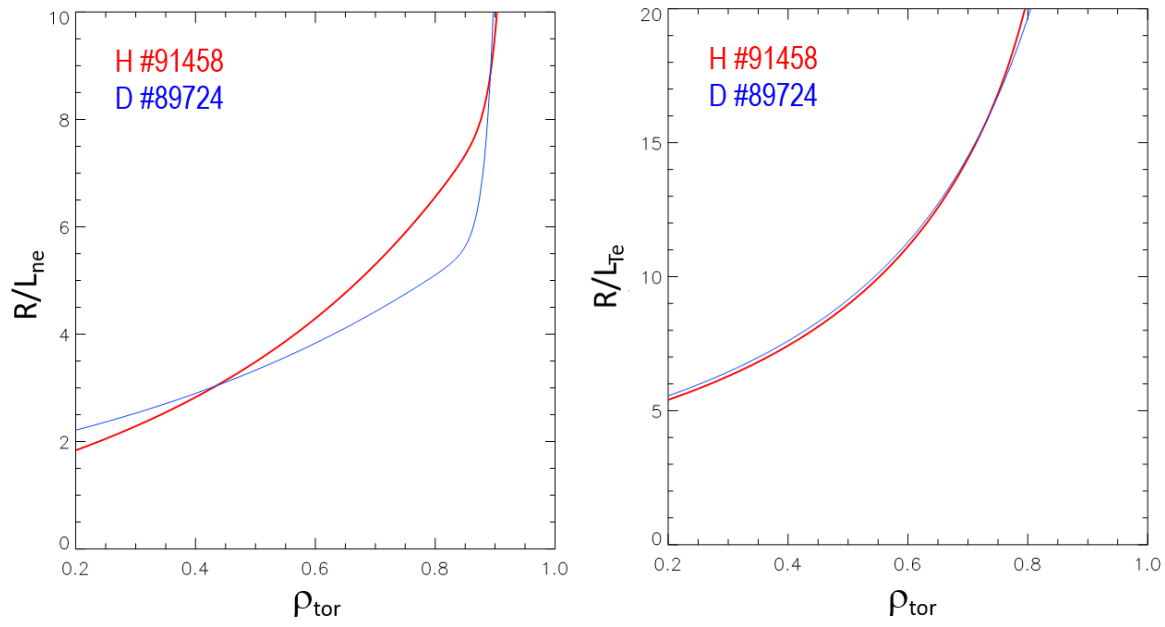

Figure 2. *Normalized electron density (left) and temperature (right) gradient lengths of the JET-ILW L-mode isotope identity pair in H (red) and D (blue) of Figure 1 vs* $\rho_{tor} = \sqrt{\Phi_N}$, *with* Φ_N *the normalized toroidal flux.*

The choice of NB energies, quoted above, with slightly lower energies in H, allowed similar scaled NB heating profiles (TRANSP/NUBEAM [10]) to be achieved in H and D, as shown in Figure 4a. Figure 4b shows that the scaled NB particle source profile is well matched in the two isotopes in the outer half of the plasma radius, while it's somewhat larger in H for $\rho_{tor} < 0.5$. The line averaged Z_{eff}, measured by visible Bremsstrahlung (with Be the main impurity), is also similar in H and D, as shown in Table 1. We thus conclude that the dimensionless identity is achieved in the L-mode core confinement region. The scaled thermal energy confinement times $B_T\ \tau_{E,th}\ /A$ and core plasma effective heat diffusivities (from TRANSP power balance), $A\ \chi_{eff}/\ B_T$, were found to be similar in H and D within experimental uncertainties, thus satisfying the confinement scale invariance principle, as shown in Table 1 and Figure 5a, respectively. For comparison, χ_{eff} normalized to the gyro-Bohm heat diffusivity χ_{GB} is plotted in Figure 5b for the H and D pair, with $\chi_{GB} = \rho_i^2\ c_s\ /\ a =$

ρ* T_i / (e B_T) [11]. Incidentally, we note that for an isotope identity pair in H and D the ratio χ_{GB} (H) / χ_{GB} (D) = 1.19, since ρ* is matched and $T_i \sim \sqrt{A}$ and $B_T \sim A^{3/4}$.

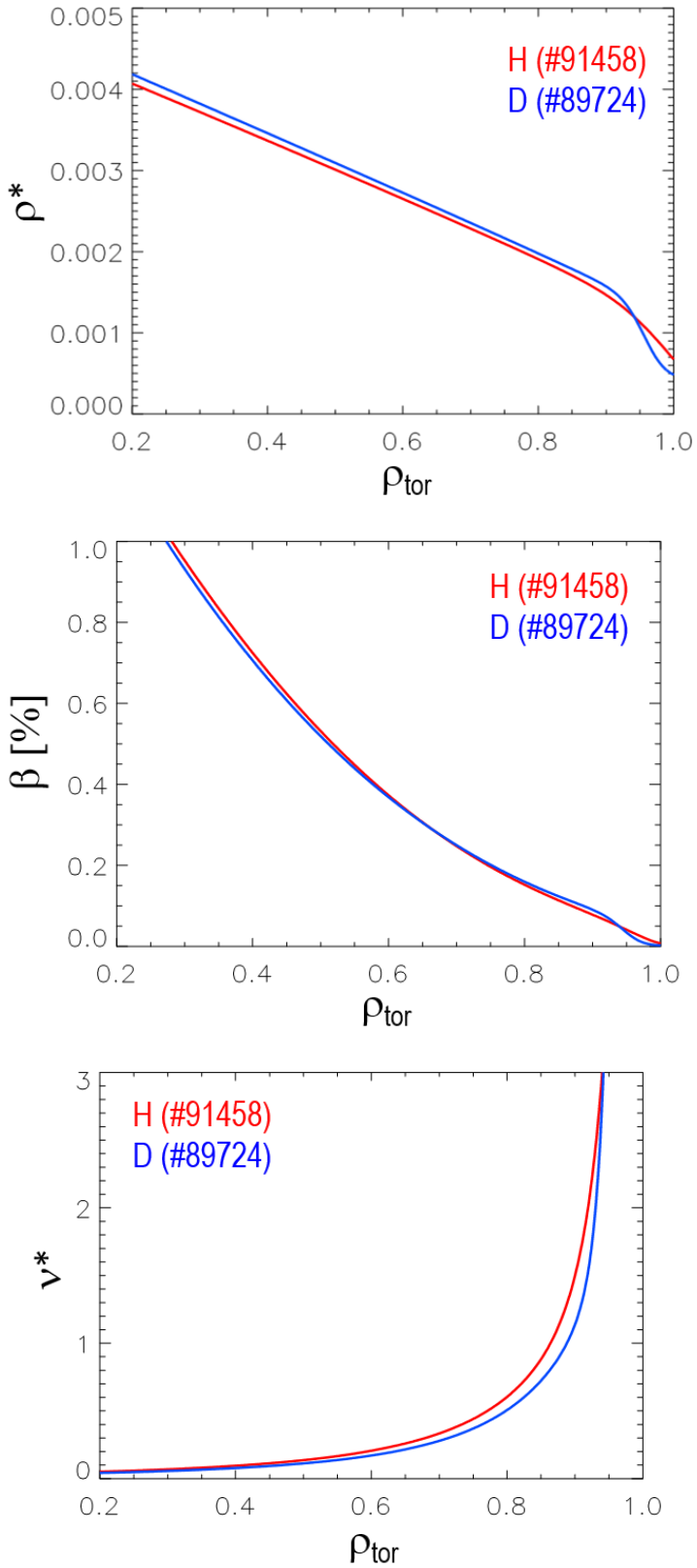

Figure 3. *ρ*, β, and ν* profiles vs ρ_{tor} for the JET-ILW L-mode isotope identity pair in H (red) and D (blue).*

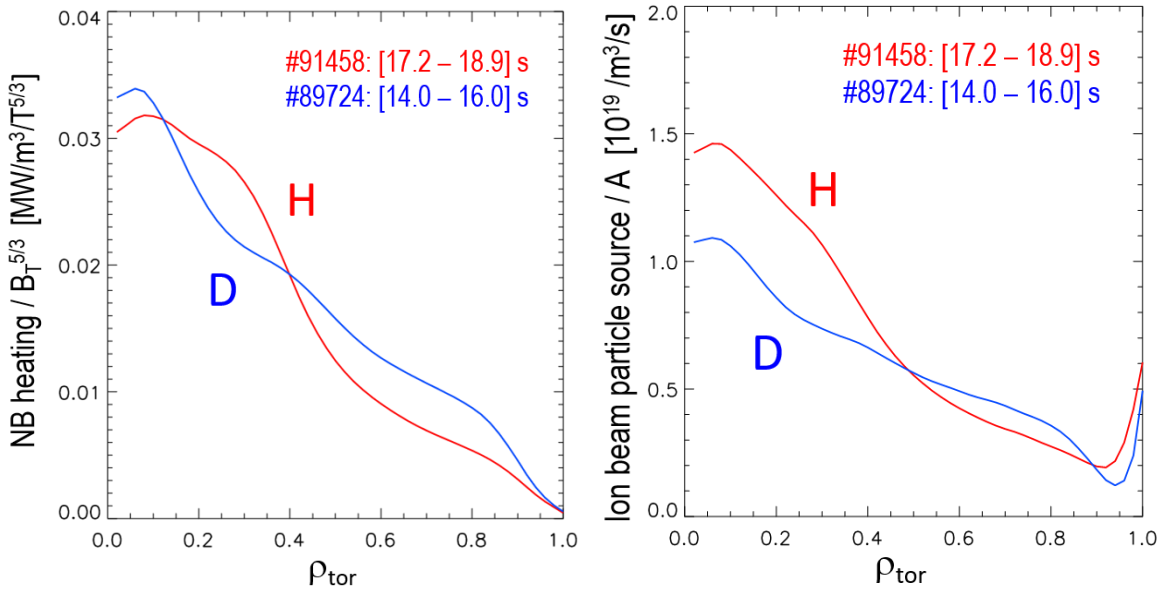

Figure 4. (a) *Scaled NB heating and (b) scaled NB particle source profiles (TRANSP/NUBEAM) for the H (red) and D (blue) L-mode isotope identity pair.*

Pulse #	**#91458**	**#89724**
Isotope	H	D
Time interval [s]	17.2 – 18.9	14.0 – 16.0
B_T [T]	1.74	2.95
I_P [MA]	1.44	2.46
P_{abs} [MW] (±10%)	2.56	6.24
$\tau_{E,th}$ [s] (±10%)	0.155	0.19
$P_{abs}/B_T^{5/3}$ [MW/T$^{5/3}$]	**1.02**	**1.03**
Z_{eff} (±10%)	**1.4**	**1.35**
T_i / T_e	**1.0**	**1.0**
$B_T\ \tau_{E,th}$ / A [T/s]	**0.27**	**0.28**

Table 1. *Main parameters of the JET-ILW L-mode isotope identity pair.*

Finally, we note a mismatch (less than a factor of 2) in Mach number $M \sim \omega_{tor}\ R\ \sqrt{m_i}\ /\sqrt{kT_e}$ (toroidal rotation velocity normalized to ion sound speed, with $v_{tor} = R\ \omega_{tor}$) between the H and D shots. For reference, the Mach number values at $\rho_{tor} = 0.5$ are $M = 0.25$ in H and $M = 0.35$ in D, respectively. However, as will be shown in Section 3 by predictive core transport modelling, the mismatch in M profiles is not significant in this case and does not invalidate the achieved dimensionless profiles identity.

The sawtooth inversion radius, obtained from the ECE diagnostic, is located at ρ_{tor} ~ 0.22 – 0.26, where q_ψ ~ 1. The scaled sawtooth frequencies were different in the JET-ILW L-mode identity pair, with $A\, f_{saw} / B_T$ = 7.5 Hz/T in H and 4.7 Hz/T in D, almost twice in H than in D. On the other hand, as noted previously in section 1, in the JET-C type I ELMy H-mode isotope identity also the scaled sawtooth frequencies were matched in H and in D [3]. In dimensional L-mode experiments in JET-C, with NBI heating (6MW) and limiter discharges (3.1MA/2.9T), f_{saw}(H) was approximately twice than f_{saw}(D) [12]. In the JET-ILW L-mode NBI power scans at constant density in H and D, at 2.5MA/3.0T, reported in [13], the sawteeth were more frequent in H than in D at low P_{NBI}, while f_{saw} became similar in the two isotopes at the highest powers in the scan (7-9 MW). These different results warrant further investigation, which is however outside the scope of this paper.

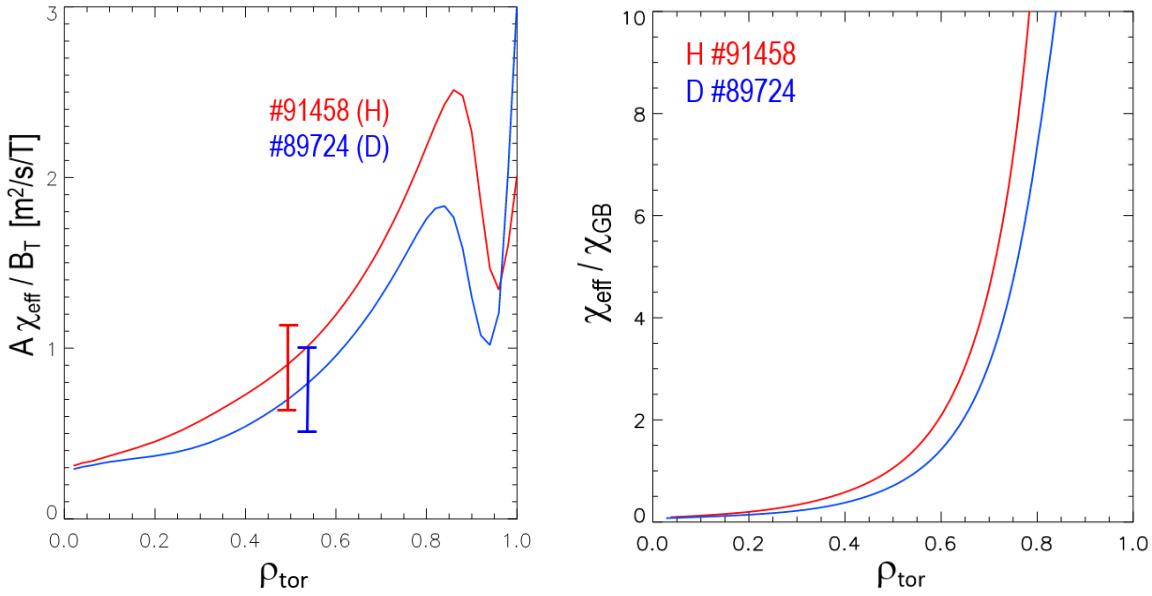

Figure 5. *Scaled effective heat diffusivity $A\chi_{eff}/B_T$ (left) and χ_{eff} normalized to χ_{GB} (right) for the L-mode isotope identity pair in H (red) and D (blue), with parameters as in Table 1.*

The scaled energy confinement times of the H and D isotope identity pair yield $\Omega_i\, \tau_{E,th} \sim A^{0.05\pm0.1}$, indicating no isotope mass dependence for the dimensionless thermal energy confinement time. We note that in order to relate the isotope mass scaling of the dimensionless thermal energy confinement time $\Omega_i\, \tau_{E,th} \sim (\rho^{*\alpha_\rho}\, \beta^{\alpha_\beta}\, \nu^{*\alpha_\nu}\, q^{\alpha q}\, A^{\alpha A,D} \ldots)$ to that of the dimensional thermal energy confinement time $\tau_{E,th} \sim (I_P^{\alpha_I}\, B_T^{\alpha_B}\, P^{\alpha_P}\, n_e^{\alpha n}\, A^{\alpha_{A,E}} \ldots)$, a transformation between scaling laws in dimensionless and dimensional variables needs to be applied (see Table 5 in [2]). The exponent of the isotope mass scaling in dimensional form is [2]:

$$\alpha_{A,E} = [1/2\ \alpha_\rho + \alpha_{A,D} + 1]/[1 - 1/2\ \alpha_\rho - \alpha_\beta + 2\ \alpha_\nu] \quad (6)$$

Therefore, evaluation of $\alpha_{A,E}$ requires knowledge of the ρ^*, β and ν^* scaling – obtained by separate dimensionless experiments - in addition to $\alpha_{A,D}$ obtained by the isotope identity experiment reported here . If, by way of example, we assume from the literature (see e.g. [2] and references therein) that the L-mode scalings are close to Bohm scaling, $\Omega_i\ \tau_{E,th} \sim \rho^{*-2}$, and that both β and ν^* scalings are weak in L-mode, namely $\alpha_\beta \sim \alpha_\nu \sim 0$, then $\alpha_{A,E} \sim 0$. This is not inconsistent with the weak, favourable isotope mass scaling of $\tau_{E,th} \sim A^{0.15\pm0.02}$ derived from the JET-ILW L-mode power scans (with NBI) at constant density in H and D [13]. In those experiments, the anomalous heat and particle diffusivities, $D_\perp$ and $\chi_\perp$, were found to be larger in H than in D only in the edge region (both inside and outside the LCFS) in interpretative EDGE2D/EIRENE simulations [13], while in the plasma core the one-fluid, effective heat diffusivity χ_{eff} ($\rho_{tor} \sim 0.5$) was comparable for H and D at all power levels of the NBI power scan at constant density [13].

3. Predictive core plasma transport modelling

Predictive core plasma transport modelling of the L-mode isotope identity pair in H and D was carried out with flux-driven JETTO-TGLF using the multi-scale saturation rule including ion and electron transport scales (SAT1) [14]. The model predictions apply to the plasma region between $\rho_{tor} = 0.8$, where the boundary conditions are set from experiment, and the sawtooth inversion radius $\rho_{tor} \sim 0.2$. No sawtooth model was used in this work. Inputs to the local, quasilinear turbulence model TGLF [15] are the local values of T_i, n_i, T_e, n_e, v_{tor} (toroidal rotation) and the local gradients, as well as local q, magnetic shear, plasma elongation and triangularity. The fluxes, generated as part of the output, are used as input to the transport code JETTO [16], [17], which solves the 1D transport equations (averaged over the magnetic surfaces) for electron and ion densities and energies in a time dependent axisymmetric MHD equilibrium configuration. Additional inputs to JETTO are the boundary conditions (from experiment in this case) and the heat and particle sources/sinks. In the simulations reported here, the NBI heat and particle sources are computed by TRANSP/NUBEAM [10]. The main output is the prediction of T_i, T_e, n_i, n_e profiles, while v_{tor} is not predicted in this case and is an input from experiment. While a single call to TGLF is a gradient-driven turbulence simulation, the coupled JETTO-TGLF runs evolve the

profiles from the initial condition provided by experiment using the fluxes computed by TGLF. In this framework, TGLF is called repeatedly until a steady state is reached (after a simulation time >> $\tau_{E,th}$). The final profiles predicted by JETTO thus represent a self-consistent flux-driven prediction of TGLF, with the fluxes in balance with the sources and sinks.

The model prediction of the L-mode isotope identity pair is in very good agreement with experiment for both isotopes, as shown in Figure 6. With fixed gradient inputs, the local TGLF model has gyro-Bohm scaling of the fluxes. However, when it is used (within JETTO) to make flux driven global predictions, the stiff core heat transport, intended here in terms of strong sensitivity of the applied heat fluxes to small variations in the core temperature gradients, which is typical of JET-ILW NBI heated L-modes and H-modes at moderate input powers (P_{NBI} < 20 MW), see e.g. [13], overcomes the local gyro-Bohm scaling ($\chi_{gB} \sim \sqrt{A}$) by the same argument laid out in [18] in the prediction of the kinetic profiles and thus of the global thermal energy confinement time (once the boundary conditions at the edge are imposed from experiment). In order words, the local gyro-Bohm scaling of core heat transport does not simplistically translate to the global energy confinement time as $\tau_{E,th} \sim a^2/\chi_{gB} \sim 1/\sqrt{A}$ (against much experimental evidence), since the heat diffusivity is not constant but strongly depends on the temperature gradient.

In the TGLF simulations reported here, Ion Temperature Gradient modes (ITGs) are found to be the dominant instabilities in the plasma core of both H and D L-modes, both at ion spatial scales ($0 < k_\theta \rho_s < 1$) - as shown by the growth rates and frequencies of the two most dominant modes - and at electron spatial scales ($k_\theta \rho_s >> 1$) – where most of the electron heat flux is found at ion scales, as indicated by the electron heat flux spectra of Figure 7. Furthermore, the ratio of (γ_ETG/k_ETG)/ (γ_ITG/k_ITG) is 0.62 for #89724 and 0.55 for #91458. Further confirmation that ITGs are the dominant instabilities in the plasma core of these isotope identity L-modes is obtained by the JETTO-TGLF power balance, which yields a ratio of ion to electron heat flux at mid-radius Q_i/Q_e (ρ_{tor} = 0.5) = 2 for the H shot (#91458) and Q_i/Q_e (ρ_{tor} = 0.5) = 2.5 for the D shot (#89724).

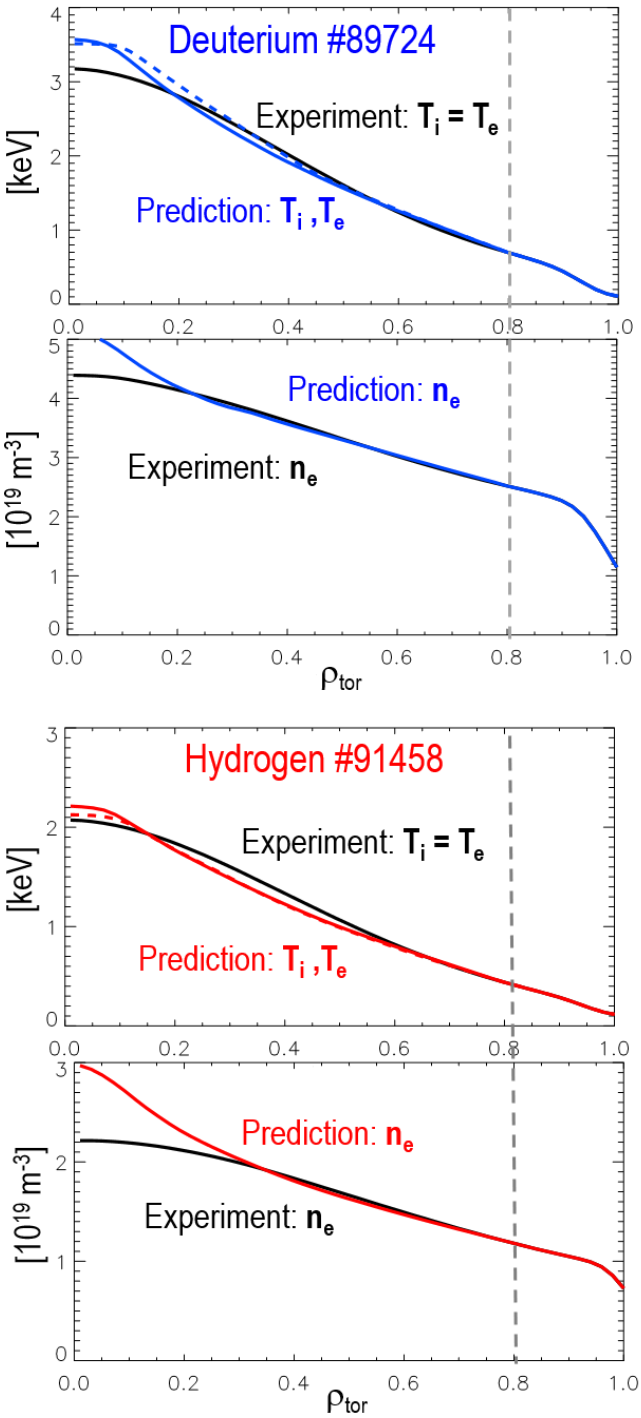

Figure 6. *JETTO-TGLF (SAT1) predicted profiles for T_e, T_i and n_e and comparison with experiment (black) for the L-mode isotope identity pair in H (red) and D (blue). The model prediction applies to the region between ρ_{tor} = 0.8 (vertical, dashed grey line), where the boundary condition is set from experiment, and the sawtooth inversion radius at ρ_{tor} ~ 0.2 (determined from ECE). T_i = T_e from experiment; predicted T_e = solid line, predicted T_i = dashed line in the JETTO-TGLF simulations. No sawtooth model was used here.*

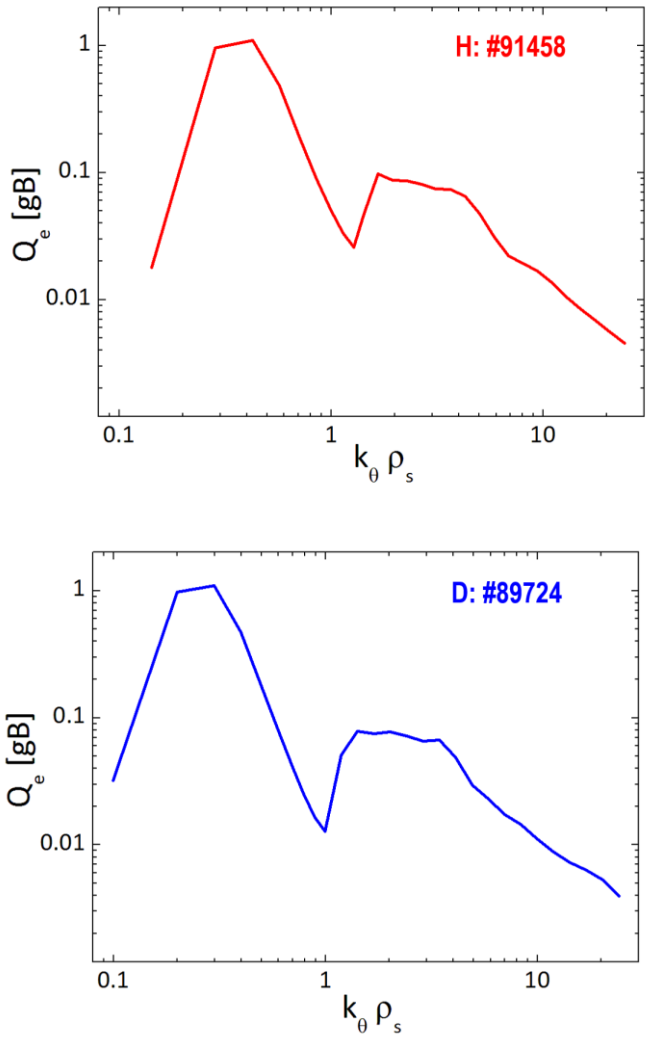

Figure 7. *Electron heat flux spectra (in gyro-Bohm units, normalized to D mass) from TGLF at ρ_{tor} = 0.56, for H (#91458) and D (#89724) L-mode shots, corroborating the finding that ITGs are the dominant instabilities in the plasma core, for both isotopes.*

Effects of collisions, toroidal rotation and and *ExB* shearing are included in the quasi-linear computations, while effects of impurities are not included. We note, however, that Z_{eff} ~ 1.4 for these plasmas, with Be the main impurity, for both H and D. Stabilization of ITG modes due to core fast ions pressure gradient is not included here, due to the low fast ion population fraction of these L-mode discharges at low NB heating levels. The JETTO-TGLF runs indicate a negligible effect of toroidal rotation v_{tor} (which is an input from experiment in this case, with v_{tor} slightly larger in D than in H) and *ExB* shearing on the predicted heat and particle transport channels of the isotope identity H and D pair, as shown in Figure 8. This is perhaps not surprising, given the low beta (β_N ~ 0.6) and low momentum input of these L-mode plasmas. Therefore, the mismatch in Mach number between the H and D

shots, quoted in Section 2, is not significant in this identity pair and does not invalidate the achieved dimensionless profiles identity.

The H and D identity pair have, by definition, very similar core density profile peaking (see Figure 1a) at same ρ^*, ν^*, β and q. As noted in Section 2, the scaled NBI particle source profile is, however, somewhat larger in H than in D for $\rho_{tor} < 0.5$. The JETTO-TGLF predictive modelling indicates that, in addition to the pinch term, the NBI particle source also contributes to the core density peaking of these L-modes, by approximately 40%, after subtraction of the edge contribution. Pure gyro-Bohm transport models predict identical density peaking R/L_n, independent of A, at zero particle flux. With collisional effects included, slightly larger density peaking – but inside typical density measurements error bars - is predicted for H than for D for ITG dominated transport [19], a result also found in the JETTO-TGLF predictive modelling reported here. This is illustrated in Figures 9a and 9b, where the predicted kinetic profiles (dashed lines) are compared with experiment (solid lines) in JETTO-TGLF simulations where the isotope mass is swapped in the transport calculations (D into H for #89724 and H into D for #91458), while boundary conditions and sources and sinks are kept from experiment. It can be seen that the predicted n_e profile for D with A = 1 (Figure 9a) is slightly more peaked than in Figure 6a, while no appreciable difference is observed in the predicted temperature profiles.

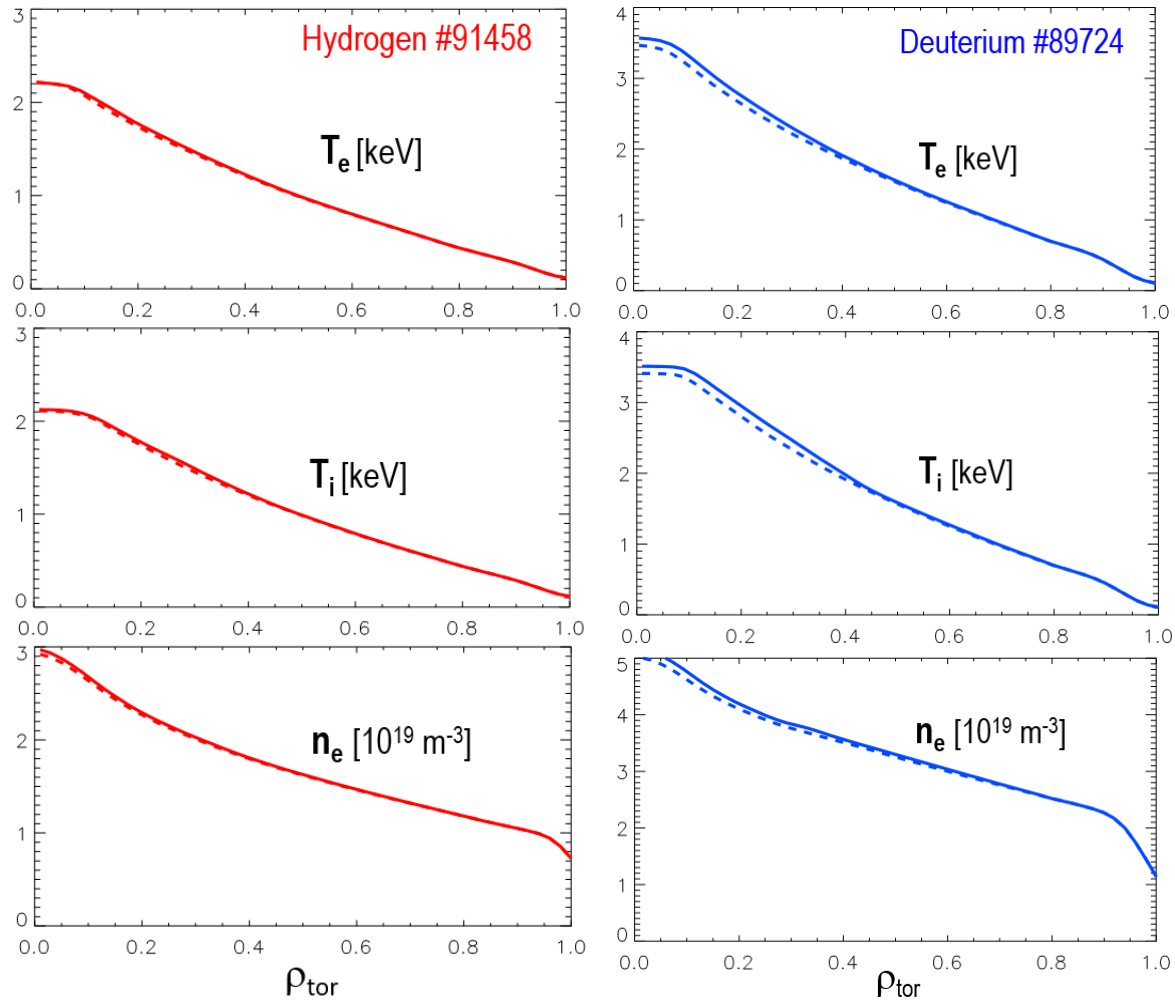

Figure 8. *JETTO-TGLF (SAT1) predicted profiles for T_e, T_i and n_e with (solid lines) and without (dashed lines) ExB shear effects – resulting from the experimentally measured v_{tor} gradients - for the H (red) and D (blue) L-mode isotope identity pair.*

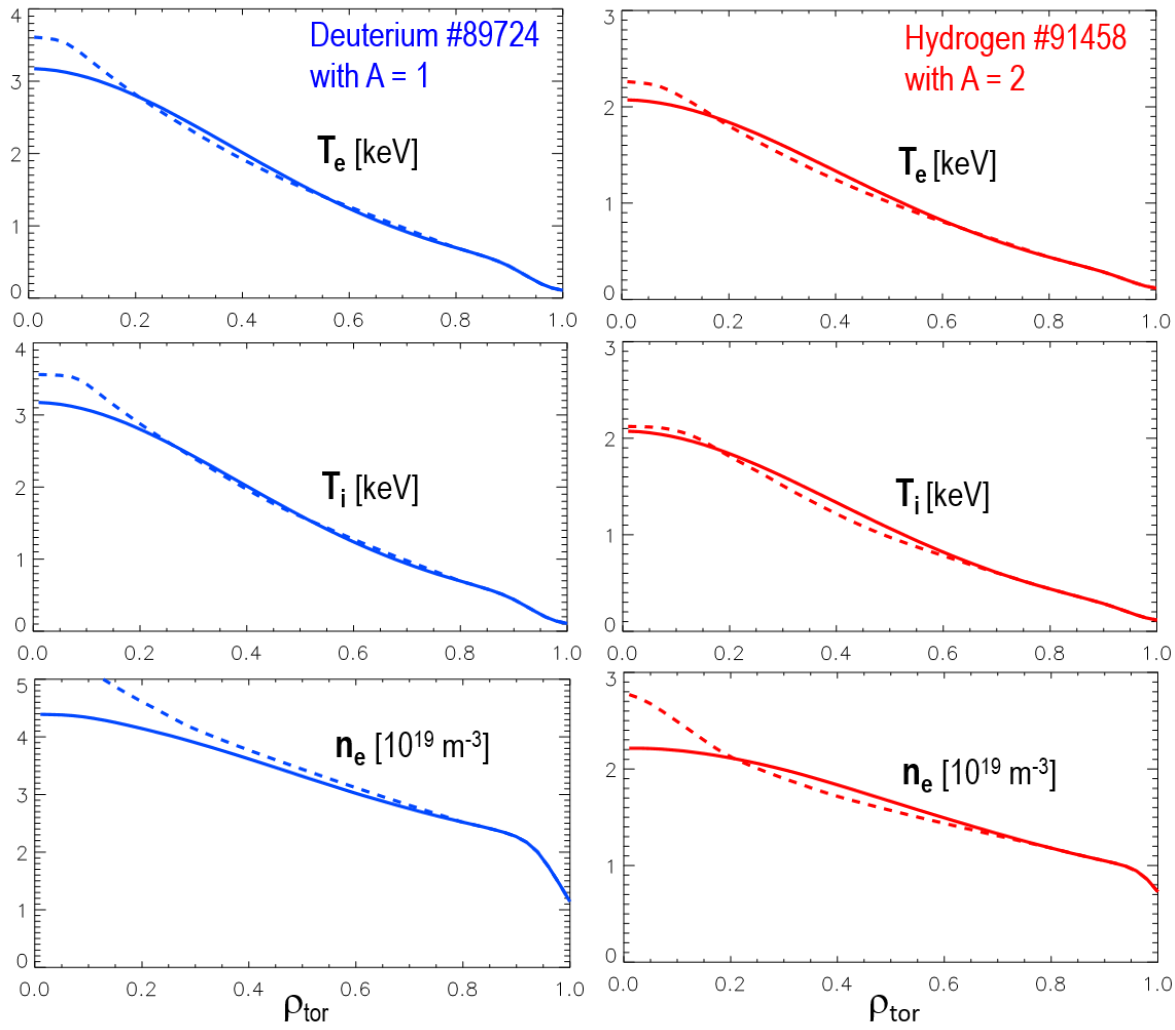

Figure 9. *T_e, T_i and n_e experimental profiles (solid lines) and JETTO-TGLF (SAT1) predicted profiles (dashed lines) where the isotope mass is swapped in the transport calculations (left: D → H and right: H → D), while boundary conditions and sources/sinks are input from experiment for H shot #91458 (red) and D shot #89724 (blue) – to be compared with the profiles of Figure 6.*

4. Conclusions and outlook

Isotope identity experiments test the validity of the confinement scale invariance principle, which is at the heart of predictive capability for fusion performance in future devices. In particular, with such experiments one can test whether the same physics is involved when varying ρ* via {B_T, T} only, as in ρ*-scaling experiments (see e.g. the review work of [2] and references therein) which are typically run in D plasmas, as opposed to via {B_T, T and A} as in the experiments of [3] in JET-C and those reported here for JET-ILW.

The studies reported in this paper have shown that NBI-heated L-mode plasmas have been obtained in JET-ILW in H and D, with matched profiles of the dimensionless plasma parameters, ρ^*, ν^*, β and q in the plasma core confinement region and same scaled energy confinement time $\Omega_i\ \tau_{E,th}$. Therefore, in this region of the plasma, where ITGs are the dominant instability, the confinement scale invariance principle is satisfied. The dimensionless thermal energy confinement time, $\Omega_i\ \tau_{E,th}$, and the scaled core plasma heat diffusivity $A\chi_{eff}/B_{T,}$ are matched in H and D, yielding $\Omega_i\ \tau_{E,th} \sim A^{0.05\pm0.1}$. Predictive modelling with JETTO-TGLF of the isotope identity pair is in very good agreement with experiment for both isotopes, for both particle and energy channels. The stiff core heat transport, which is typical of JET-ILW NBI heated L-modes, such as those of this study, overcomes the local gyro-Bohm scaling of gradient-driven TGLF, explaining the absence of isotope mass dependence of the dimensionless thermal energy confinement time $\Omega_i\ \tau_{E,th}$. The effect of *ExB* shearing on the predicted heat and particle transport channels is found to be negligible for these low beta and low momentum input plasmas (while this effect may instead be sizeable in high power H-modes, see e.g. [20]), hence the mismatch in the *M* number profile does not invalidate the isotope identity in this case.

An isotope identity in H and D had been achieved in the type I ELMy H-mode regime in JET with C-wall, remarkably throughout the entire plasma radius. In the L-mode isotope identity reported in this paper, density and temperature measurements with HRTS are not available inside the sawtooth inversion radius ($\rho_{tor} \sim 0.2$). However, the scaled density profiles from LIDAR [21] and temperature profiles from ECE [22], which extend radially inwards to $\rho_{tor} = 0$, are very similar in H and D, indicating that the isotope identity may also have been achieved in the plasma centre. In this region, though, the scaled sawtooth frequency is not matched, being almost twice in H than in D, unlike in the JET-C isotope identity in H-mode. As the volume of the sawtooth dominated region is small compared to that of the confinement region, it has little impact on the global energy confinement time, which, together with core plasma transport, is the focus of this work. We're also not venturing here to explore whether the H and D scaled edge kinetic profiles are matched near the last closed flux surface (LCFS) and in the SOL, as this goes beyond the accuracy of the available measurements for this H & D pair in this plasma region, where HRTS signal statistics becomes poor and the ECE diagnostic spatial resolution is inadequate to resolve the temperature gradient (and, in addition, transition to optically thin plasma makes the T_e profile from ECE unreliable in this region). On the other hand, the narrow

edge layer just inside and outside the LCFS is the crucial one where isotope dependencies may occur in L-mode transport, in particular for the particle channel in JET-ILW, as discussed in [13]. This is the subject of further, ongoing study and has important implications for the understanding of the isotope dependence of the L-H power threshold and of H-mode pedestal transport.

In ELMy H-modes, isotope identity experiments must also demonstrate the profile match in the pedestal region, which strongly influences the global energy confinement for stiff core heat transport. Moreover, the evidence from JET-ILW is that the strong, favourable isotope mass dependence of $\tau_{E,th}$ in type I ELMy H-modes originates at the pedestal [13]. As mentioned in Section 1, conditions at the plasma boundary, such as influx of neutral particles across the LCFS and into the edge transport barrier, may introduce additional physics, so that the canonical plasma physics parameters may no longer be sufficient to describe the plasma transport properties. This could potentially invalidate the approach of the confinement scale invariance principle. To explore these issues, isotope identity experiments were also performed in H and D type I ELMy H-modes in JET-ILW. However, further optimization of the profiles matches is sought in the upcoming JET campaign and these studies will be reported in a future work.

Last, but not least, planned JET-ILW experiments in T are crucial, not only to add a 3rd isotope to the dataset (by far a non-trivial experimental achievement per se), but because the physics underlying the 'isotope effect' is complex and non-linear: it involves interaction between the local scales, where gradient driven instabilities arise, and global scales, where stiff heat transport and density profile peaking are important. As T plasmas are expected to have similar or better confinement than D, and not worse as in H [13], studying D and T means focussing on the fusion-relevant isotope pair. We also stress again that the physics mechanisms that play a role in explaining the isotope mass dependence of L-mode core transport, such as those discussed in this paper, are not necessarily the same as those responsible for explaining core transport in high power H-modes. An obvious example is the effect of shear rate, which is predicted to reduce transport as the isotope mass is increased: the instabilities growth rate is reduced as $\gamma_{max} \sim 1/\sqrt{A}$, for fixed profile shapes [18], [23], [20]. Therefore, the stabilizing effect of *ExB* shear should be assessed realistically in conjunction with the profile shape effects as the isotope mass is changed in experiment.

Acknowledgments: *This work was carried out within the framework of the EUROfusion Consortium and received funding from the Euratom research and training programme 2014–2018 under grant agreement No. 633053 and from the RCUK Energy Programme grant No. EP/P012450/1. The views and opinions expressed herein do not necessarily reflect those of the European Commission. The authors are grateful to Drs Clive Challis, Yann Camenen and Martin Valovic for very useful discussions.*

References:

[1] Connor J W and Taylor J B 1977 *Nucl. Fusion* **17** 1047

[2] Luce T C *et al.* 2008 *Plasma Phys. Control. Fusion* **50** 043001

[3] Cordey J G *et al.* 2000 *Plasma Phys. Control. Fusion* **42** A127

[4] Brezinsek S *et al.* 2013 *Nucl. Fusion* **53** 083023

[5] Cordey J G *et al.* 1999 *Nucl. Fusion* **39** 301

[6] Pasqualotto R *et al.* 2004 *Rev. Sci. Instrum***. 75** 3891

[7] Delabie E *et al. 25th IAEA FEC* (2014) EX/P5-24, *St Petersburg, Russia*

[8] Nunes I et al. *26th IAEA FEC* (2016), *Kyoto, Japan, EXC-P8*

[9] Menmuir S *et al.* 2014 Rev. *Sci. Instrum.* **85** 11E412

[10] Goldston R J *et al.* 1981 *J. Comput. Phys.* **43** 61

[11] Garbet X *et al.* 2019 *Nucl. Fusion* **50** 043002

[12] Tibone F *et al.* 1993 *Nucl. Fusion* **33** 1319

[13] Maggi C F *et al.* 2018 *Plasma Phys. Control. Fusion* **60** 014045

[14] Staebler G *et al.* 2017 *Nucl. Fusion* **57** 66046

[15] Staebler G *et al.* 2007 *Phys. Plasmas* **14** 055909

[16] Cenacchi G and Taroni A, JET-IR(88)03, 1988

[17] Romanelli M *et al.* 2014 *Plasma and Fusion Research* **9** 3403023

[18] Bateman G *et al.* 1999 *Phys. Plasmas* **6** 4607

[19] Angioni C *et al.* 2018 *Phys. Plasmas* **25** 082517

[20] Garcia J *et al.* 2017 *Nucl. Fusion* **57** 014007

[21] Maslov M *et al.* 2013 *JINST* **8** C11009

[22] De la Luna E *et al.* 2004 *Rev. Sci. Instrum.* **75** 3831

[23] Scott S *et al*. 1996 *Proc. 16th Fusion Energy Conf. vol 1, (Montreal)* p 573